Solar Energy Materials & Solar Cells 160 (2017) 60–66

Contents lists available at ScienceDirect

Solar Energy Materials & Solar Cells

journal homepage: www.elsevier.com/locate/solmat

High-temperature shaping perovskite film crystallization for solar cell fast preparation

Jiajiu Ye[a,b], Haiying Zheng[a], Liangzheng Zhu[a], Xuhui Zhang[a], Ling Jiang[a], Wangchao Chen[a], Guozhen Liu[a,b], Xu Pan[a,*], Songyuan Dai[c,*]

[a] Key Laboratory of Novel Thin-Film Solar Cells, Institute of Applied Technology, Hefei Institutes of Physic Science, Chinese Academy of Sciences, Hefei 230031, China

[b] University of Science and Technology of China, Hefei 230026, China

[c] State Key Laboratory of Alternate Electrical Power System with Renewable Energy Sources, North China Electric Power University, Beijing 102206, China

ARTICLE INFO

Keywords:
High-temperature treatment
Perovskite crystallization
Fast preparation

ABSTRACT

Recent developments of PSCs have achieved great progress with power conversion efficiency reached to 22.1%. The crystal growth process as an important factor will significantly influence the quality of perovskite films and the device performance. In this paper, we demonstrate a simple approach for fast preparation based on the precursor compositions of $(FAPbI_3)_{0.85}(MAPbBr_3)_{0.15}$ by regulating the temperature during annealing process for transition from FAI, PbI_2, MABr, and $PbBr_2$ to perovskite. The film will be shaped in 15 s for one-step deposition at annealing temperature of 220 °C. It has been found that higher temperature will induce perovskite to form larger size and oriented crystal grains rapidly. This will contribute to longer carrier lifetime and smaller carrier recombination which, are beneficial for solar cell device. The champion cell with PCE of 17.1% had been obtained measured under conditions of AM 1.5 G, 100 mW/cm^2. Furthermore, this method exhibits good stability which is benefited from large size crystal, the device will not be deteriorated and the PCE maintained over 90% after 3 months.

1. Introduction

Organic-inorganic perovskite and its derivatives as a new branch of solar cells have achieved rapid development since miyasaka and co-workers reported perovskite solar cells (PSCs) for the first time in 2009 [1–7]. In the past few years, PSCs have shown rapid progress due to the high power conversion efficiency (PCE) and relatively low potential cost. Park et al. reported Spiro-OMeTAD as HTM used in solid state organic/inorganic perovskite solar cells (PSCs) and got photoelectric conversion efficiency of 9.7% [8]. In last year, seok's team used intramolecular exchange process (IEP) technique to induce perovskite to form crystals by PbI_2-DMSO reacting with FAI and got 20.1% power conversion efficiency. This certified record was refreshed up to 22.1% until today [9].

Despite such a rapid progress in perovskite solar cells [10–13], many issues about efficiency and stability in the light-harvesting process still remain unclear. The intrinsic property of the metal-halide perovskite was proposed as a fundamental factor influencing the performance. The poor morphology of the perovskite thin film, trap states at surface, interstitial defects in crystal lattice, recombination between charge carriers, and the crystallization process during the growth of the perovskite thin films not only cause electrical shorting but also harm charge carriers transportation. In order to increase devices performance and avoid energy loss, researchers focus their attention on making dense and low defects perovskite layer with high quality crystallization.

A large number of recent successes on lead halide perovskite solar cells are observed in solution processed thin films due to their facile fabrication and several strategies have been used to control the crystallization processes. Adjustment of precursor solution [14], additives like HX [15], gas-assisted method [16], microwave irradiation process [17], and laser-assisted crystallization [18] have been used for nucleation and to promote growth of the perovskite crystals. The effect of crystallization conditions, especially temperature has an important impact on the morphology of the perovskite films. The effect of temperature and annealing time on the perovskite crystal formation have lot of reports, ranging from 90 °C to 130 °C and from 20 to 90 min respectively. Liu's team had reported that higher temperature will produce perovskite films ($MAPbI_3$) not only got better crystallinity and larger grain size, but also better photovoltaic performance with a PCE

* Corresponding authors.
E-mail addresses: xpan@rntek.cas.cn (X. Pan), sydai@ipp.ac.cn (S. Dai).

http://dx.doi.org/10.1016/j.solmat.2016.10.022
Received 18 July 2016; Received in revised form 2 October 2016; Accepted 9 October 2016
Available online 24 October 2016
0927-0248/

of 12.9% prepared at 200 °C and heated for 6 min [19]. But the most commonly used lead halide perovskite of $MAPbI_3$ has a lower thermal decomposition temperature, and the decomposition process can be further accelerated by high temperature [20–22]. Due to the thermal stability obstacle, high temperature treatment of lead halide perovskite film crystallization for fast preparation only has scarcely studies [23–25]. In this aspect, a higher thermal decomposition material $(FAPbI_3)_x(MAPbBr_3)_{1-x}$ is desired to resist heating destruction, which will enable perovskite films can be subjected to high temperature treatment owing to improved stability of intrinsic perovskite absorber layer and much higher formation energies [26,27].

The conventional thermal annealing process transfers energy into the as-prepared perovskite film is from bottom to up, which retards the evaporation of the solvent and makes the grains grow gradually. In contrast, high-temperature provides a simple and straight forward way to define the crystal orientation, unit cell volume and grain size. Compared with conventional annealing method which usually produces more defects with small crystal grain, perovskite films treated by high temperature always have slightly larger grain size which could render low trap density and excellent charge-carrier diffusion length. This can effectively reduce carrier recombination rate, and at the same time improve the carrier mobility and charge carrier collection efficiency [28–30]. All of this will deliver decent power conversion efficiency (PCE).

In this work, we demonstrate a simple approach for fast preparation method at annealing temperature of 220 °C, and the film will be shaped in 15 s. The precursor composition was changed from $MAPbI_3$ to $(FAPbI_3)_{0.85}(MAPbBr_3)_{0.15}$ for one-step deposition. The effects of high-temperature treatment on the crystallinity, morphology of perovskite film and associated photovoltaic performance were systematically investigated. Results showed that higher annealing temperature would accelerate transition rate from FAI, PbI_2, MABr, and $PbBr_2$ to $(FAPbI_3)_{0.85}(MAPbBr_3)_{0.15}$ and produce perovskite film with better crystallinity, enhanced crystal orientation and larger crystal grain, which was further confirmed by an XRD analysis. The TAS results showed that the carrier lifetime increased from 200.6 to 440.1 ns by high temperature treatment. The largest crystal grains around 800 nm had been produced at 220 °C, which delivered a highest PCE of 17.1%. In addition the as-prepared perovskite solar cell have higher stability. The device without any encapsulation did not deteriorate with the PCE maintaining over 90% for 3 months after its preparation while the device prepared by conventional method only held 3 weeks.

2. Experimental

2.1. Materials

Lead (II) Iodide (99.99%, trace metals basis) [for Perovskite precursor] was purchased from TCI, CH_3NH_3I from Xi'an Polymer Light Technology Corp., TiO_2 (particle size: about 30 nm, crystalline phase: anatase) TiO_2 from dysol. DMF, chlorobenzene, lithium bis (trifluoromethylsulphonyl) imide (Li-TFSI) and 4-tert-butylpyridine (tBP) from Aldrich, and spiroMeOTAD from Borun New Material Technology Co., Ltd. All chemicals were directly used without further purification. Patterned FTO-coated glass substrates with a sheet resistance of 15 $\Omega\,sq^{-1}$ were cleaned sequentially by ultrasonication in mild detergent, deionized water, acetone and ethanolamine. The substrates were exposed to UV-ozone for 20 min prior to the spin coating step.

2.2. Solar cell device fabrication

A thick dense blocking layer of TiO_2 (bl-TiO_2) was deposited onto F-doped SnO_2 (FTO) substrate by spin coating to prevent direct contact between the FTO and the hole-conducting layer. A TiO_2 blocking layer was deposited on the cleaned FTO by spray pyrolysis, using dry air as carrier gas, at 460 °C from a precursor solution of 0.6 ml of titanium diisopropoxide and 0.4 ml of bis (acetylacetonate) in 7 ml of anhydrous isopropanol. A mesoporous TiO_2 layer (dysol, particle size: about 30 nm, crystalline phase: anatase, diluted to w/w=1/6 in ethanol) about 160–180 nm thickness film was deposited by spin coating at 4000 rpm for 20 s onto the bl-TiO_2/FTO substrate. After spin coating, the substrate was immediately dried on a hotplate at 80 °C, and the substrates were then calcined at 500 °C to remove organic components. The perovskite film was deposited by spin coating onto the TiO_2 substrate. The prepared FAI powders and PbI_2 (TCI) for 1.2 M $(FAPbI_3)_{0.85}(MAPbBr_3)_{0.15}$ solution were stirred in a mixture of DMSO and DMF (v/v=8:2) at 60 °C for completely dissolved. The resulting solution was coated onto the mp-TiO_2/bl-TiO_2/FTO substrate by a consecutive two-step spin-coating process at 1100 and 5000 r.p.m for 20 s and 30 s respectively. During the second spin-coating step at last 10 s, the substrate was treated with weak corrosive mixed anti-solvent (chlorobenzene1) to form the perovskite crystal, and the substrate was then heated at 220 °C for 15 s on a hotplate under low speed flow clean dry air. Then quickly transferred to the aluminum plate for radiating to prevent the film from continuous overheating. When the temperature decreased to 80–100 °C, annealing at 105 °C for another 5 min. (The conventional method was that the film coated with perovskite precursor was directly heated at 100 °C for 1 h). FAI was synthesized from hydroiodic acid reacting with formamidine acetate according to reference. The HTM layer was deposited by spin-coating at 4000 rpm for 20 s, using a solution of spiroMeOTAD, 4-tert-butylpyridine, and lithium bis (trifluoromethylsulphonyl) imide and the Co (III)-complex. Finally, Gold (80 nm) counter electrode was deposited by thermal evaporation on top of the device to form the back contact.

2.3. Characterization

The PCE and *J–V* curves were measured by using a solar simulator (Newport, Oriel Class A, 91195A) with a source meter (Keithley 2420) at 100 mA/cm^2 illumination AM 1.5 G and a calibrated Si-reference cell certified by NREL. The *J–V* curves for all devices were measured by masking the active area with a black mask 0.09 cm^2. UV–vis absorption spectra were recorded on a UV–vis spectrometer (Hitachi U-3300). Incident photon to current efficiency (IPCE) were confirmed as a function of wavelength from 300 to 800 nm (PV Measurements, Inc.), with dual Xenon/quartz halogen light source, measured in DC mode with no bias light used. The setup was calibrated with a certified silicon solar cell (Fraunhofer ISE) prior to measurements. Film morphology was investigated by using a high-resolution scanning electron microscope equipped with a Schottky Field Emission gun. PL spectra were recorded by exciting the perovskite films deposited onto mesoporous TiO_2 at 490 nm with a standard 450 W Xenon CW lamp. The signal was recorded by a spectrofluorometer (photon technology international) and analyzed by the software Fluorescence. X-ray diffraction spectra of the perovskite films were recorded on an X'Pert MPD PRO (PANalytical). The data were collected at room temperature in the 2θ range 10–50°. The automatic divergence slit (10 mm) and beam mask (10 mm) were adjusted to the dimension of the films. A baseline correction was applied to all X-Ray thin film diffractograms to compensate for the broad feature arising from the FTO glass and anatase substrate. Transient absorption spectra (TAS) was record on LKS (Applied photophysics). The cells were measured before evaporating gold counter with a pump light wavelength of 500 nm and a probe light wavelength of 760 nm. Repetition rate of 5 Hz, the energy of laser device is 150 μJ/cm^2.

3. Result and discussion

Fig. 1 depicted the preparation process, the precursor solution was spin-coated on the TiO_2 substrate to form perovskite layer followed by

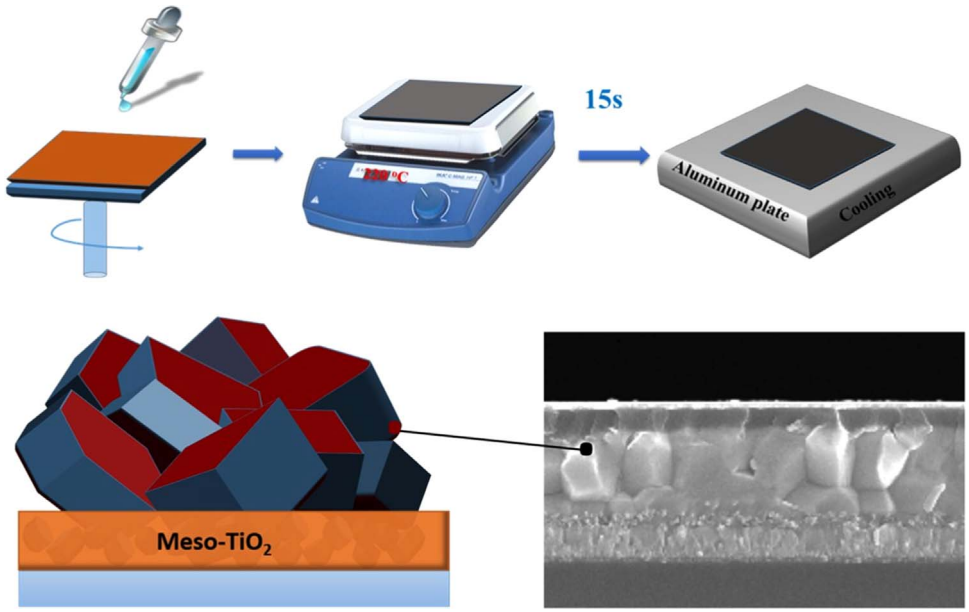

Fig. 1. Schematic of high temperature treatment for Perovskite solar cell rapid preparation and large particles crystals prepared by high temperature-induced method. Low temperature aluminum as heat transfer plate to prevent the film from continuous heating.

thermal annealing around 220 °C for 15 s to complete the perovskite crystal formation. Then, the film was quickly moved to low temperature heat transfer plate to prevent the film from continuous heating. Thermal stability perovskite capping layer was formed due to enhanced cohesion in crystal lattice. In additional, the benefit of the approach can also act as templates to direct nucleation or crystal growth, which would help film to form a uniform surface morphology and big size grain.

The morphology of perovskite film based on one-step solution deposition method was mainly governed by nucleation and crystal growth. When the perovskite film landed on the hot substrate for annealing, the solvents quickly evaporated and the perovskite began to nucleating and crystallizing. Generally, rapid nucleation and slow crystal growth were promising ways to obtain perovskite films of high optoelectronic quality. We introduced high temperature annealing as a method for crystal engineering of perovskite. It could enable heterogeneous nucleation which was believed to be orders of magnitude faster than the homogeneous nucleation. This was attributed to continuously supplying heat was far more than the nucleation free energy barrier [31,32]. Therefor it resulted in smooth perovskite films with fewer defects and larger oriented grains.

In order to check the effect of temperature on the perovskite formation, XRD measurement has been conducted to monitor this process. XRD patterns of $MAPbI_3$ and $(FAPbI_3)_{0.85}(MAPbBr_3)_{0.15}$ films annealing at 220 °C for 15 s, the $MAPbI_3$ film was decomposed obviously (Fig. S1), the XRD peak located at 12.6° which is assigned to (001) of the PbI_2 becomes stronger while (110) peak (belongs to perovskite) becomes weaker. It indicates that formamidine perovskite film has a higher decomposition temperature. The films of $(FAPbI_3)_{0.85}(MAPbBr_3)_{0.15}$ annealing at 160 °C, 180 °C, 200 °C, 220 °C and 240 °C for 15 s respectively, as illustrated in Fig. 2(a), PbI_2 gradually transformed into perovskite and all the perovskite films exhibited strong diffraction peaks at 14.1°, 28.4° and 31.9°, which can be indexed to the (110), (220) and (310) planes of the perovskite crystal (β- phase) [33]. Compound of PbI_2 was completely converted to perovskite at 220 °C, and the diffraction peaks almost cannot be detected. But the transition from $(FAPbI_3)_{0.85}(MAPbBr_3)_{0.15}$ to PbI_2 was significantly observed while annealing temperature increasing from 220 to 240 °C, indicating the partially decomposition of the perovskite film. Additionally, an increase of diffraction intensity ratio between (110) and (310) indicated that the orientation of perovskite crystal was

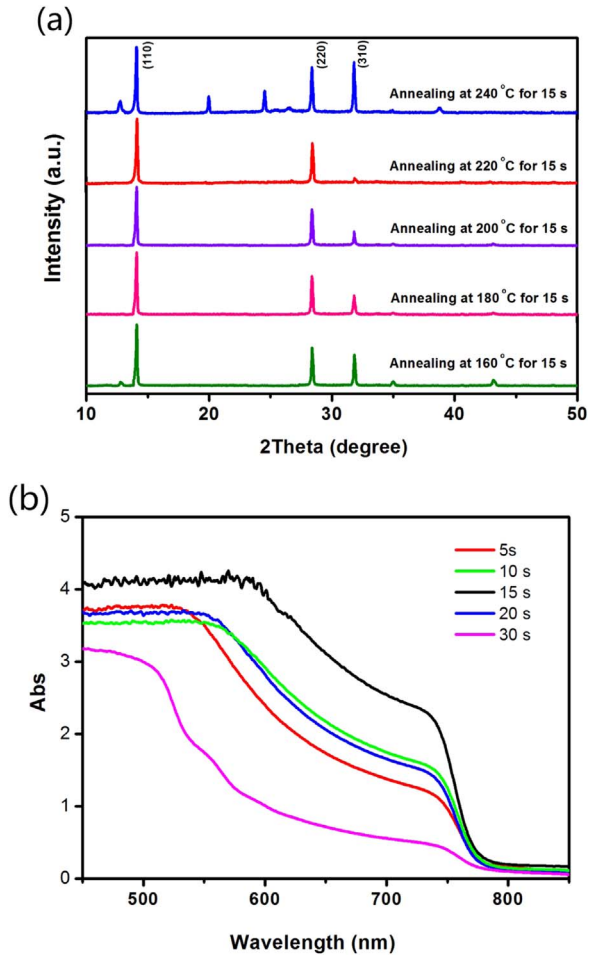

Fig. 2. (a) XRD patterns of perovskite films deposited on glass substrate treated by different temperature (b) UV absorption of perovskite film annealing at different time deposited on meso-TiO_2/bl-TiO_2/FTO substrates.

enhanced with increasing temperature. The result clearly showed that the intensity of (110) and (220) peaks were very strong compared to other peak, demonstrating better crystallization of perovskite film which is good for optoelectronic device performance. The perovskite films were annealing at 220 °C for 10 s, 20 s, 30 s and 60 s (Fig. S2). Parts of PbI_2 had not transformed into perovskite completely which can be ascribed to the insufficient crystallization when the heating time is only 5 s. Along with the heating time increased to 30 s, an additional peak at 12.6° related to PbI_2 still can be observed in the XRD pattern, which means the partially decomposition and leads to the descent of crystallinity. The perovskite films of pure $(FAPbI_3)_{0.85}(MAPbBr_3)_{0.15}$ were formed under high temperature treatment for 15 s, indicating the remaining solvent will evaporate in less than 15 s. The fast evaporation of solvent accelerated the crystallization as well as directed nucleation or crystal growth which would lead to the higher quality of perovskite film.

The optical absorption of pristine films annealing at 220 °C were investigated by UV–vis spectrometers as shown in Fig. 2(b), there was a notable increase in the absorbance in 15 s, probably due to the increased PbI_2 conversion to perovskite at higher speed and better crystallinity; after 20 s, the absorbance had a significantly decrease which should be ascribed to perovskite decomposition, and this result correlated with the XRD data.

In order to have a comprehensive understanding of temperature influence on the crystallization, the surface and sectional morphology of perovskite films were investigated by scanning electron microscopy (SEM) which were prepared by conventional one-step deposition annealing at 100 °C and high temperature treatment at 160 °C, 220 °C respectively. The corresponding results are shown in Fig. 3, a series of clear changes have taken place on the films. As exhibited in Fig. 3(a) and (c), perovskite thin film prepared at 100 °C with the crystal size around 200 nm. The sectional crystal boundary was not clearly and most area was blur, indicating poor crystallize. As temperature increased to 160 °C, the crystal grains and boundary were observed more clearly with grain size increased gradually. More heat energy was provided to improve the crystallization of the pristine film at 220 °C. Therefore, the flatter surface and arranged crystal grains were formed with the maximum diameter of 800 nm shown in Fig. 3(b) and (d), indicating higher reaction temperature will produce larger crystal grains and less grain boundaries. The crystallinity of perovskite

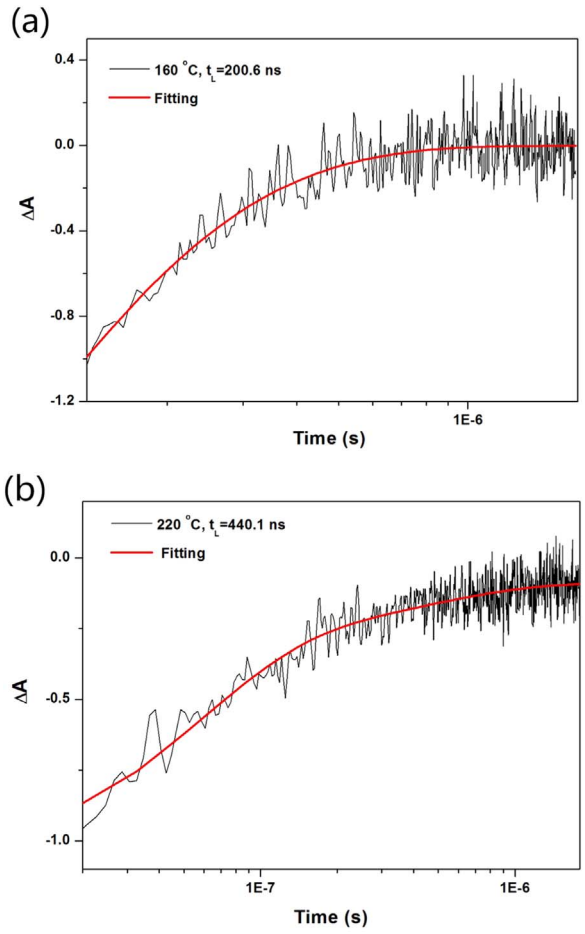

Fig. 4. TAS response of perovskite film deposit on glass substrate treated with different annealing temperature (160 °C, 180 °C, 200 °C, 220 °C), charge carries lifetime (t_L) was simulated by LKS (produced by Applied photophysics). The test were measured with a pump light wavelength of 500 nm and a probe light wavelength of 760 nm. The red solid line represents the fitting result with bi-exponential function. (For interpretation of the references to color in this figure legend, the reader is referred to the web version of this article.)

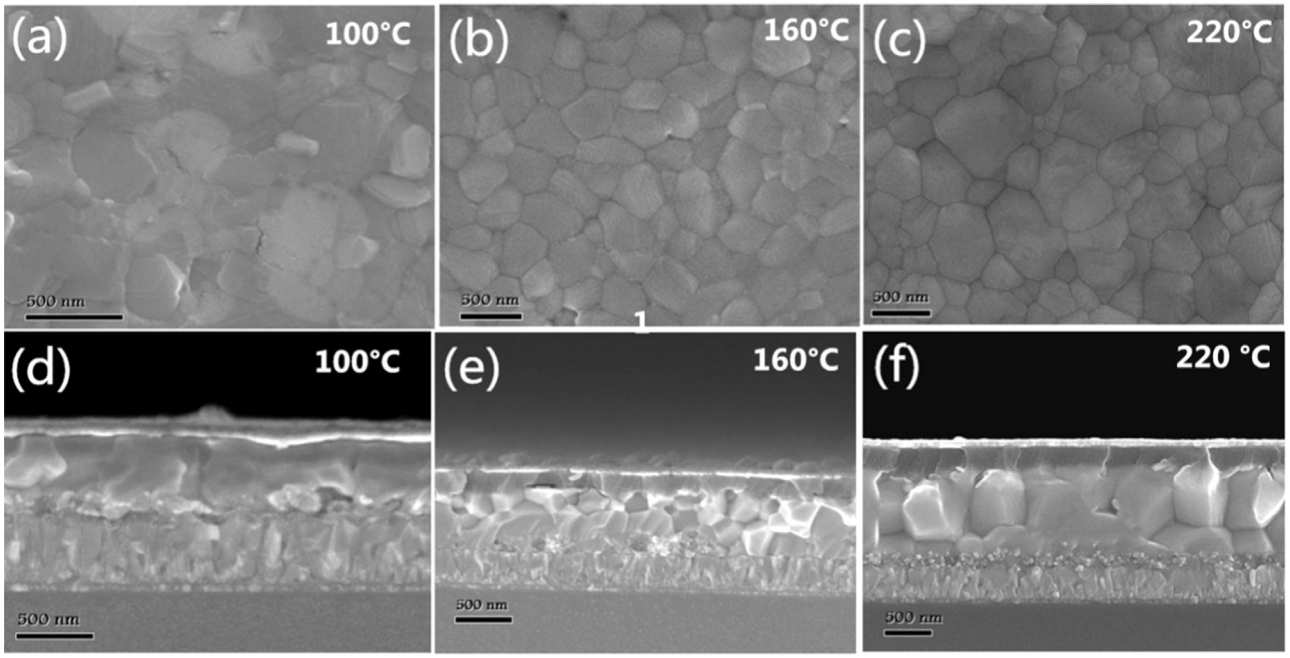

Fig. 3. The surface morphology and cross sectional SEM images of perovskite solar cells prepared at different temperature, (a) and (d) 100 °C, (b) and (e) 160 °C, (c) and (f) 220 °C.

films was closely related to the device performance , which has already been confirmed. The benefits of larger crystal could be arose from the following aspects: (1) reduced charge trapping and recombination (2) enhanced grain orientation of the perovskite film and charge carrier collection efficiency (3) reduced grain boundary and enhanced intrinsic stability of the perovskite itself.

For the purpose of further understanding the effect of high temperature on the light absorbing layer, transient absorption spectra (TAS) was used to detect the electron and hole recombination signal. As shown in Fig. 4, The TAS spectrum have been measured from film side which was deposited on the glass. The electrons and holes were generated while the perovskite film under laser excitation and a large bleaching signal was observed, which was considered as the recombination of electrons and holes due to no electron injection to electron transfer layer. If the recombination of electrons and holes occurred difficultly, the longer of charge carrier lifetimes will be got [34–36]. In other words, the perovskite layer with a longer charge carries life time represents higher quality film. By fitting the TA decay with bi-exponential, we found that the decay processes existed a lifetime of 200.6 ns at 160 °C. As increasing the temperature, the charge carrier life become longer. At annealing temperature of 220 °C, the electronic life significantly increased to 440.1 ns probably ascribe to larger crystal and reduced grain boundary. A faster decay process appeared in the TA response when the film treated with 240 °C, only got 151.3 ns (Fig. S4). This may be resulted from interactions of multiple charge carrier recombination and the decomposition of PbI_2 which generated a lot of defect states traps. Additionally, a sharp decrease decay process was observed, only got 29.9 ns (Fig. S4) when perovskite deposited on the TiO_2/FTO/glass substrate. This is because electrons will inject into the quencher layer and only a small part contribute to carries life time, thus resulting in non-significant TAS signal results.

To demonstrate the feasibility of high temperature induced crystallization in the actual devices, we prepared devices with structure of FTO/compact TiO_2/meso-TiO_2/$(FAPbI_3)_{0.85}$ $(MAPbBr_3)_{0.15}$/HTM/Au. The current density-voltage curves of devices were shown in Fig. 5, and photovoltaic parameters were summarized in the inset table. The perovskite film treated with 160 °C that was fabricated by conventional anti-solvent method showed a J_{sc} of 18.90 mA/cm^2, V_{oc} of 0.97, fill factor (FF) of 70.6%, and a total PCE of 12.94%. Typically, as annealing temperature increased to 220 °C, the average grain size increased up to 800 nm. At the same time the photovoltaic parameters of devices showed significant increases. The devices demonstrate a J_{sc} of 20.93 mA/cm^2, V_{oc} of 1.05 V, and *FF* of 75.5%, corresponding to the PCE of 16.59%. The improvement of device performance mainly

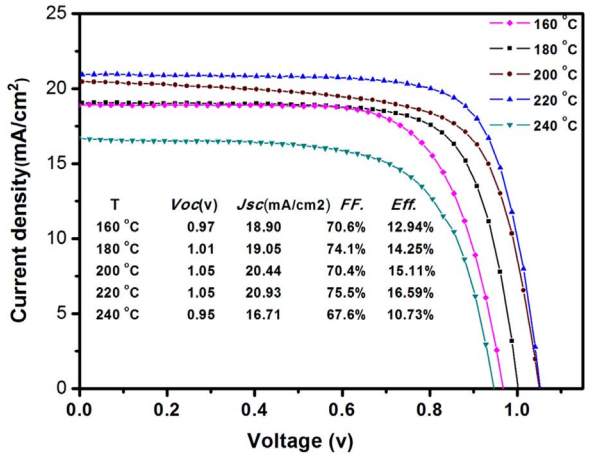

Fig. 5. The photovoltaic performance of the devices prepared by different annealing temperature (160 °C, 180 °C, 200 °C, 220 °C, 240 °C) were measured under simulated AM 1.5 G (100 mW/cm^2) solar irradiation in air, which was calibrated using a certified monocrystalline silicon solar cell.

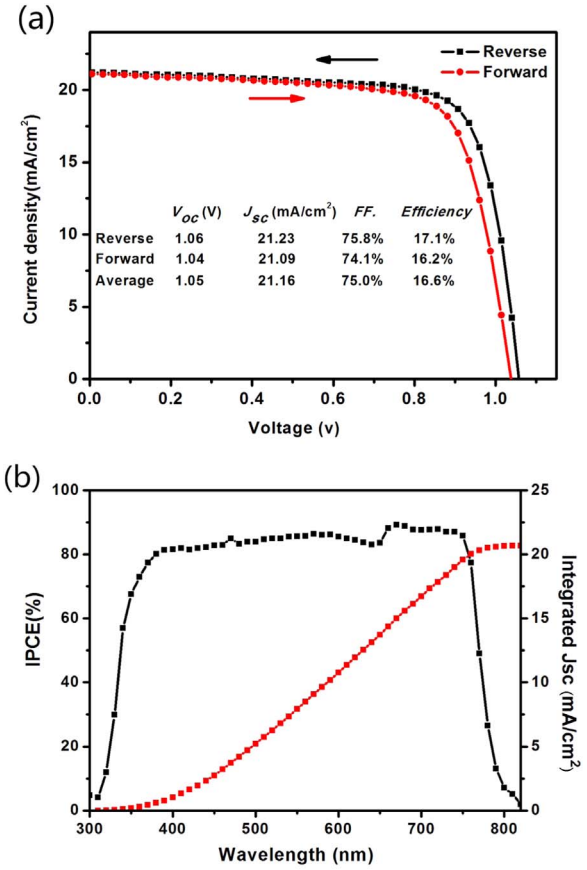

Fig. 6. *J-V* and IPCE characteristics for the best cell obtained in this study. (a) *J-V* curves of forward and reverse bias sweep for the solar cell (b) corresponding incident photon-to-current conversion efficiency (IPCE) and integrated J_{sc} spectra.

reflected in the rise of J_{sc} and V_{oc}. This can be explained as light absorption improved and charge carrier recombination reduced caused by the improved crystallization, and it will enable the devices to have higher light-harvest capability and generate more carries effectively. However, if temperature increased further to 240 °C, the device showed a PCE of 10.73%, with J_{sc}, V_{oc}, and *FF* of 16.71 mA/cm^2, 0.95 V and 67.6%, respectively. While the temperature increasing to 260 °C, the PCE reduced further and only remained 7.7% (Fig. S5) due to the limited thermal stability of the perovskite films. In addition, as annealing time increased from 15 s to 30 s at 220 °C, the PCE reduced rapidly apparently due to the partially decomposed of perovskite, which leading to the descent of crystallinity and film cracks.

30 devices have been fabricated and characterized, and the parameters of V_{oc}, J_{sc}, *FF* and PCE were plotted as a function of temperature (as shown in Fig. S6), indicating higher reproducibility and stability. Our results demonstrate that high performance devices can be easily obtained ascribe to high quality crystallinity. The performance of the best device leads to a PCE of 17.1% shown in Fig. 6(a), and the device showed an average PCE of 16.6% with J_{sc} of 21.16 mA/cm^2, V_{oc} of 1.05 V, and FF of 75.0%. The forward and backward scan results shows smallest difference, indicating less hysteresis. The calculated photocurrent from IPCE was 20.79 mA/cm^2 which was in close agreement with these measurements.

The high quality of oriented crystal perovskite films gives the devices a better photoelectric performance as well as remarkably stability. The device exhibited slower deterioration rate, and the performance of device kept over 90% which was stored in dry air and dark conditions after 3 months. However, the conventional devices showed rapidly deterioration with PCE dropping 5% after 9 days and 10% after 21 days as depicted in Fig. 7. Especially in the humidity and

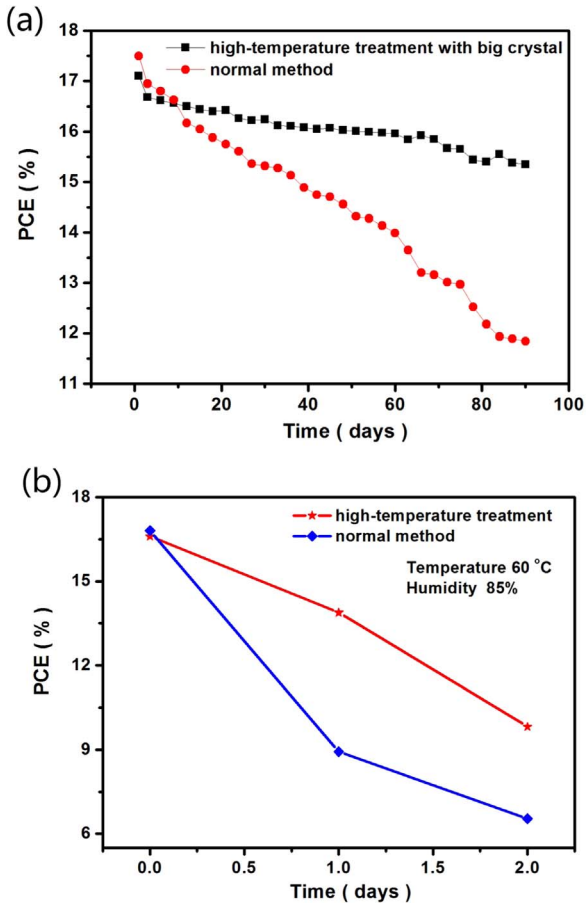

Fig. 7. The performance of perovskite solar cell prepared by high-temperature treatment and normal method. (a) Power conversion efficiency as a function of storage time in dry air and dark conditions for the perovskite solar cell with different method, the test time interval was three days (b) two type devices was stored in Humidity Chamber under the condition: temperature of 600 °C and humidity of 85%.

high-temperature environment (60 °C, relative humidity around 85%), the device treated by high temperature showed significant superiority probably due to stone-like big size crystal and excellent crystallinity, and this will result perovskite itself have strong ability to resist decomposition. The as-prepared device can hold the PCE of 80% in the first day and 60% in the second day. However the device made by conventional method deteriorated in 24 h and only remained half of PCE.

4. Conclusions

In summary we have demonstrated a fast preparation method for PSCs with annealing temperature at 220 °C for one-step deposition, and the film will be shaped in 15 s. We use the precursor compositions of $(FAPbI_3)_{0.85}(MAPbBr_3)_{0.15}$ owing to higher thermal stability of intrinsic perovskite absorber layer compared with $MAPbI_3$ precursor compositions. The perovskite film can be successfully shaped by high temperature annealing process to form larger size and oriented crystal grains. This would contribute to longer carrier lifetime and smaller carrier recombination as well as lead to a better performance of devices. The best device with a PCE of 17.1% had been obtained prepared at 220 °C and got average PCE of 16.6% with J_{sc} of 21.16 mA/cm^2, V_{oc} of 1.05 V, and FF of 75.0%. Furthermore, the results show that this method not only improves the overall photo-electric performance, but also exhibits good stability. The device without any encapsulation did not deteriorate with the PCE maintaining over 90% after 3 months. Especially in humidity and high-temperature environment, the as-prepared device can hold the PCE of 80% in the first day and 60% in the second day, yet the device made by conventional method which only remained half of PCE. Further work on the study and employment of increasing the thermal and humidity stability of perovskite is on progress.

Acknowledgements

This work was financially supported by the National High Technology Research and Development Program of China under Grant no. 2015AA050602, the National Natural Science Foundation of China under Grant no. 21273242, and State Key Laboratory of Alternate Electrical Power System with Renewable Energy Sources (Grant no. LAPS14012). Science and Technology Support Program of Jiangsu Province under Grant no. BE2014147-4.

Appendix A. Supporting information

Supplementary data associated with this article can be found in the online version at doi:10.1016/j.solmat.2016.10.022.

References

[1] J. Burschka, N. Pellet, S.-J. Moon, R. Humphry-Baker, P. Gao, M.K. Nazeeruddin, M. Grätzel, Sequential deposition as a route to high-performance perovskite-sensitized solar cells, Nature 499 (2013) 316–319.
[2] B. Conings, L. Baeten, T. Jacobs, R. Dera, J. D'Haen, J. Manca, H.-G. Boyen, An easy-to-fabricate low-temperature TiO2 electron collection layer for high efficiency planar heterojunction perovskite solar cells, APL Mater. 2 (2014) 081505.
[3] N.J. Jeon, J.H. Noh, Y.C. Kim, W.S. Yang, S. Ryu, S.I. Seok, Solvent engineering for high-performance inorganic–organic hybrid perovskite solar cells, Nat. Mater. 13 (2014) 897–903.
[4] H. Zhou, Q. Chen, G. Li, S. Luo, T.-b. Song, H.-S. Duan, Z. Hong, J. You, Y. Liu, Y. Yang, Interface engineering of highly efficient perovskite solar cells, Science 345 (2014) 542–546.
[5] D. Liu, J. Yang, T.L. Kelly, Compact layer free perovskite solar cells with 13.5% efficiency, J. Am. Chem. Soc. 136 (2014) 17116–17122.
[6] L. Zhu, Z. Shao, J. Ye, X. Zhang, X. Pan, S. Dai, Mesoporous BaSnO3 layer based perovskite solar cells, Chem. Commun. 52 (2016) 970–973.
[7] W. Fu, J. Yan, Z. Zhang, T. Ye, Y. Liu, J. Wu, J. Yao, C.-Z. Li, H. Li, H. Chen, Controlled crystallization of CH 3 NH 3 PbI 3 films for perovskite solar cells by various PbI2 (X) complexes, Sol. Energy Mater. Sol. Cell 155 (2016) 331–340.
[8] H.-S. Kim, C.-R. Lee, J.-H. Im, K.-B. Lee, T. Moehl, A. Marchioro, S.-J. Moon, R. Humphry-Baker, J.-H. Yum, J.E. Moser, Lead iodide perovskite sensitized all-solid-state submicron thin film mesoscopic solar cell with efficiency exceeding 9%, Sci. Rep. 2 (2012) 591.
[9] N.J. Jeon, H.G. Lee, Y.C. Kim, J. Seo, J.H. Noh, J. Lee, S.I. Seok, o-Methoxy substituents in spiroOMeTAD for efficient inorganic–organic hybrid perovskite solar cells, J. Am. Chem. Soc. 136 (2014) 7837–7840.
[10] W. Li, J. Fan, J. Li, Y. Mai, L. Wang, Controllable grain morphology of perovskite absorber film by molecular self-assembly toward efficient solar cell exceeding 17%, J. Am. Chem. Soc. 137 (2015) 10399–10405.
[11] T.A. Berhe, W.-N. Su, C.-H. Chen, C.-J. Pan, J.-H. Cheng, H.-M. Chen, M.-C. Tsai, L.-Y. Chen, A.A. Dubale, B.-J. Hwang, Organometal halide perovskite solar cells: degradation and stability, Energy Environ. Sci. 9 (2016) 323–356.
[12] Y. Kumar, E. Regalado-Pérez, A.M. Ayala, N. Mathews, X. Mathew, Effect of heat treatment on the electrical properties of perovskite solar cells, Sol. Energy Mater. Sol. Cells 157 (2016) 10–17.
[13] L. Zhao, X. Wang, X. Li, W. Zhang, X. Liu, Y. Zhu, H.-Q. Wang, J. Fang, Improving performance and reducing hysteresis in perovskite solar cells by using F8BT as electron transporting layer, Sol. Energy Mater. Sol. Cells 157 (2016) 79–84.
[14] D. Bi, W. Tress, M.I. Dar, P. Gao, J. Luo, C. Renevier, K. Schenk, A. Abate, F. Giordano, J.-P.C. Baena, Efficient luminescent solar cells based on tailored mixed-cation perovskites, Sci. Adv. 2 (2016) e1501170.
[15] G. Li, T. Zhang, Y. Zhao, Hydrochloric acid accelerated formation of planar CH3NH3PbI3 perovskite with high humidity tolerance, J. Mater. Chem. A 3 (2015) 19674–19678.
[16] F. Huang, Y. Dkhissi, W. Huang, M. Xiao, I. Benesperi, S. Rubanov, Y. Zhu, X. Lin, L. Jiang, Y. Zhou, Gas-assisted preparation of lead iodide perovskite films consisting of a monolayer of single crystalline grains for high efficiency planar solar cells, Nano Energy 10 (2014) 10–18.
[17] Q. Cao, S. Yang, Q. Gao, L. Lei, Y. Yu, J. Shao, Y. Liu, Fast and controllable crystallization of perovskite films by microwave irradiation process, ACS Appl. Mater. Interfaces 8 (2016) 7854–7861.
[18] F. Li, W. Zhu, C. Bao, T. Yu, Y. Wang, X. Zhou, Z. Zou, Laser-assisted crystallization of CH3NH3PbI3 films for efficient perovskite solar cells with a high open-circuit voltage, Chem. Commun. 52 (2016) 5394–5397.
[19] X. Ren, Z. Yang, D. Yang, X. Zhang, D. Cui, Y. Liu, Q. Wei, H. Fan, S.F. Liu, Modulating crystal grain size and optoelectronic properties of perovskite films for

solar cells by reaction temperature, Nanoscale 8 (2016) 3816–3822.
[20] E.S. Parrott, R.L. Milot, T. Stergiopoulos, H.J. Snaith, M.B. Johnston, L.M. Herz, Effect of structural phase transition on charge-carrier lifetimes and defects in CH3NH3SnI3 perovskite, J. Phys. Chem. Lett. 7 (2016) 1321–1326.
[21] X. Guo, C. McCleese, C. Kolodziej, A.C. Samia, Y. Zhao, C. Burda, Identification and characterization of the intermediate phase in hybrid organic–inorganic MAPbI 3 perovskite, Dalton Trans. 45 (2016) 3806–3813.
[22] Z. Li, M. Yang, J.-S. Park, S.-H. Wei, J. Berry, K. Zhu, Stabilizing perovskite structures by tuning tolerance factor: formation of formamidinium and cesium lead iodide solid-state alloys, Chem. Mater. 28 (2015) 284–292.
[23] W. Nie, H. Tsai, R. Asadpour, J.-C. Blancon, A.J. Neukirch, G. Gupta, J.J. Crochet, M. Chhowalla, S. Tretiak, M.A. Alam, High-efficiency solution-processed perovskite solar cells with millimeter-scale grains, Science 347 (2015) 522–525.
[24] Q. Cao, S. Yang, Q. Gao, L. Lei, Y. Yu, J. Shao, Y. Liu, Fast and controllable crystallization of perovskite films by microwave irradiation process, ACS Appl. Mater. Interfaces 8 (2016) 7854–7861.
[25] Z. Zang, A. Nakamura, J. Temmyo, Single cuprous oxide films synthesized by radical oxidation at low temperature for PV application, Opt. Express 21 (2013) 11448–11456.
[26] R. Shang, S. Chen, B.W. Wang, Z.M. Wang, S. Gao, Temperature-induced irreversible phase transition from perovskite to diamond but pressure-driven back-transition in an ammonium copper formate, Angew. Chem. Int. Ed. 55 (2015) 2097–2100.
[27] B. Wang, K.Y. Wong, S. Yang, T. Chen, Crystallinity and defect state engineering in organo-lead halide perovskite for high-efficiency solar cells, J. Mater. Chem. A 4 (2016) 3806–3812.
[28] B. Yang, O. Dyck, J. Poplawsky, J. Keum, A. Puretzky, S. Das, I. Ivanov, C. Rouleau, G. Duscher, D. Geohegan, Perovskite solar cells with near 100% internal quantum efficiency based on large single crystalline grains and vertical bulk heterojunctions, J. Am. Chem. Soc. 137 (2015) 9210–9213.
[29] L. Gouda, R. Gottesman, S. Tirosh, E. Haltzi, J. Hu, A. Ginsburg, D.A. Keller, Y. Bouhadana, A. Zaban, Vapor and healing treatment for CH3NH3PbI3−xClx films toward large-area perovskite solar cells, Nanoscale 8 (2016) 6386–6392.
[30] H. Back, G. Kim, J. Kim, J. Kong, T.K. Kim, H. Kang, H. Kim, J. Lee, S. Lee, K. Lee, Achieving long-term stable perovskite solar cells via ion neutralization, Energy Environ. Sci. 9 (2016) 1258–1263.
[31] A. Cacciuto, S. Auer, D. Frenkel, Onset of heterogeneous crystal nucleation in colloidal suspensions, Nature 428 (2004) 404–406.
[32] D. Bi, C. Yi, J. Luo, J.-D. Décoppet, F. Zhang, Shaik M. Zakeeruddin, X. Li, A. Hagfeldt, M. Grätzel, Polymer-templated nucleation and crystal growth of perovskite films for solar cells with efficiency greater than 21%, Nat. Energy 1 (2016) 16142.
[33] Q. Dong, Y. Yuan, Y. Shao, Y. Fang, Q. Wang, J. Huang, Abnormal crystal growth in CH 3 NH 3 PbI 3− x Cl x using a multi-cycle solution coating process, Energy Environ. Sci. 8 (2015) 2464–2470.
[34] Q. Shen, Y. Ogomi, J. Chang, S. Tsukamoto, K. Kukihara, T. Oshima, N. Osada, K. Yoshino, K. Katayama, T. Toyoda, Charge transfer and recombination at the metal oxide/CH 3 NH 3 PbCll 2/spiro-OMeTAD interfaces: uncovering the detailed mechanism behind high efficiency solar cells, Phys. Chem. Chem. Phys. 16 (2014) 19984–19992.
[35] A. Marchioro, J. Teuscher, D. Friedrich, M. Kunst, R. Van De Krol, T. Moehl, M. Grätzel, J.-E. Moser, Unravelling the mechanism of photoinduced charge transfer processes in lead iodide perovskite solar cells, Nat. Photo 8 (2014) 250–255.
[36] C. Wehrenfennig, G.E. Eperon, M.B. Johnston, H.J. Snaith, L.M. Herz, High charge carrier mobilities and lifetimes in organolead trihalide perovskites, Adv. Mater. 26 (2014) 1584–1589.